

See discussions, stats, and author profiles for this publication at: <https://www.researchgate.net/publication/6707378>

Magnetite-Loaded Carrier Erythrocytes as Contrast Agents for Magnetic Resonance Imaging

ARTICLE *in* NANO LETTERS · DECEMBER 2006

Impact Factor: 13.59 · DOI: 10.1021/nl0618501 · Source: PubMed

CITATIONS

106

READS

114

9 AUTHORS, INCLUDING:



Radostina Georgieva

Charité Universitätsmedizin Berlin

41 PUBLICATIONS 952 CITATIONS

[SEE PROFILE](#)



Susanne Mueller

Charité Universitätsmedizin Berlin

62 PUBLICATIONS 804 CITATIONS

[SEE PROFILE](#)



Ulf Teichgräber

Friedrich Schiller University Jena

268 PUBLICATIONS 1,895 CITATIONS

[SEE PROFILE](#)



Hans Bäuml

Charité Universitätsmedizin Berlin

92 PUBLICATIONS 2,213 CITATIONS

[SEE PROFILE](#)

Magnetite-Loaded Carrier Erythrocytes as Contrast Agents for Magnetic Resonance Imaging

M. Brähler,^{*,†} R. Georgieva,[‡] N. Buske,[§] A. Müller,[†] S. Müller,^{||} J. Pinkernelle,[⊥] U. Teichgräber,[⊥] A. Voigt,[†] and H. Bäumler[†]

Institute of Transfusion Medicine, Charité-Universitätsmedizin Berlin, Charitéplatz 1, 10117 Berlin, Germany, Max-Planck Institute of Colloids and Interfaces, Magnetic Fluids, Köpenicker Landstrasse 203, D-12437 Berlin, Germany D-14476 Golm/Potsdam, Germany, Neurologische Klinik und Poliklinik, Charité-Universitätsmedizin Berlin, Germany, and Department of Radiology, CVK, Charité-Universitätsmedizin Berlin, Germany

Received August 8, 2006; Revised Manuscript Received September 25, 2006

ABSTRACT

Superparamagnetic iron oxide nanoparticles (SPIONs) are commonly used in magnetic resonance imaging (MRI), but their fast phagocytosis makes them less than ideal for this application. To circumvent the lymphocyte–macrophage system, we encapsulated SPIONs into red blood cells (RBCs). For loading, the RBC's membrane was opened by swelling under hypoosmotic conditions and subsequently resealed. In this work, we demonstrate that SPIONs can be loaded into RBCs in a concentration sufficient to obtain strong contrast enhancement in MRI.

Contrast agents are indispensable in magnetic resonance imaging (MRI), improving its sensitivity and/or specificity. The susceptibility to the magnetic field strongly depends on the nature of the applied substances. Generally, contrast enhancement is achieved by application of para- or superparamagnetic materials to the investigated tissues and organs. For angiographic studies and for detection of focuses of inflammation paramagnetic contrast agents like gadolinium, chelates are used widely. For tissue-specific imaging, the application of gadolinium chelates are limited because this would involve ingestion of gadolinium into the cells, and free gadolinium is toxic. The blood pool half-life time of gadolinium-based contrast agents is approximately 90 min. They are eliminated from the body through the kidney.¹

The most important superparamagnetic contrast agents are iron oxide based. They consist of single-domain magnetic particles. In the absence of magnetic field, the orientation of the domains is random and the net magnetic moment is zero. An applied external magnetic field causes the magnetic dipoles to reorient according to the field, which results in a magnetic moment five times higher than that of paramagnetic substances. Both the longitudinal (T1) and transverse (T2) relaxation times are reduced.^{2,3} Superparamagnetic iron oxide

nanoparticles can be fabricated with a diameter of 3–20 nm. Uncoated iron oxide nanoparticles are usually recognized immediately and eliminated in the liver. A variety of surface modifications have been developed to increase their circulation time. For example, dextran and citrate coatings lead to an enhanced half-life time in the body of up to 1.5 h.^{4,5} Nevertheless, they are normally used as specific contrast agents for tissues with a high phagocytosis activity like the liver^{6,7} because of the recognition by lymphocyte–macrophage system is still fast.⁸ The incorporated iron oxide shows no toxicity in the administered doses. After degradation of the particles, the iron is accumulated in the body's iron stores.^{4,9}

The aim of this work is to extend the circulation time in the blood stream loading the SPIONs into red blood cells. Under physiological conditions, the permeability of the RBC membrane is highly selective. Only ions, small sugar molecules, and water can permeate through the membrane. Macromolecules can only pass the membrane through pores in the lipid bilayer artificially generated by osmotic swelling, electroporation, or chemical treatment. Under suitable conditions, this process is reversible, which means the pores can be resealed. Substances that have been loaded into the RBCs are then trapped inside. It has been shown already that RBCs can be loaded with a wide variety of substances, for example, methotrexate, L-asparaginase, and systemic corticosteroids.^{10,11} The procedure can also be exploited for loading nanoparticles into RBCs because SPIONs have a size comparable to the

* Corresponding author. E-mail: myriam.braehler@charite.de.

[†] Institute of Transfusion Medicine.

[‡] Max-Planck Institute of Colloids and Interfaces.

[§] Magnetic Fluids.

^{||} Neurologische Klinik und Poliklinik, Charité-Universitätsmedizin Berlin.

[⊥] Department of Radiology, CVK, Charité-Universitätsmedizin Berlin.

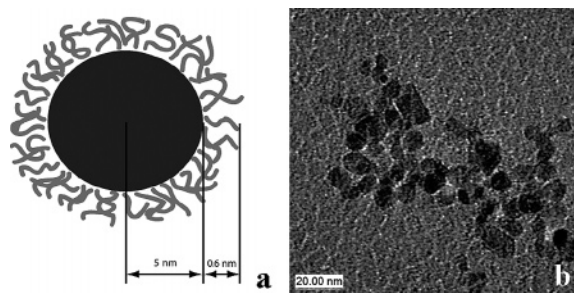


Figure 1. (a) Sketch and (b) transmission electron microscopy (TEM) image of citrate-coated magnetite nanoparticles. For the TEM, the nanoparticle suspension was diluted in aqua dest., ultrasonicated, deposited on a carbon film, and examined by means of a Philips CM 20 FEG. (Thanks to Mr. M. Röder, INNOVENT e.V., Jena).

size of many macromolecules. Loaded RBCs would have the great advantage of being biocompatible, biodegradable, and showing similar *in vivo* survival times of up to 120 days as native RBCs.^{12,13} As a contrast agent with a long circulation time, they could be used for outcome control after surgery, to monitor healing processes in blood vessels, and to detect internal bleeding.

For this study, we used SPIONs coated with citrate (Citrat MF 130905, K^+ = counterion, 5.8 wt % Fe_3O_4). The magnetite cores were coprecipitated from a mixture of 0.05 M $FeCl_2 \cdot 4H_2O$ and 0.1 M $FeCl_3 \cdot 6H_2O$ by adding 25% ammonia (Merck, Darmstadt, Germany) under moderate stirring. The dispersion was stirred at 75 °C for 30 min in order to achieve magnetite crystal formation. The obtained black particles were magnetically separated and washed up to eight times with distilled water to remove ammonium chloride. After stabilization of the magnetite hydrosol at pH 1–2 using hydrochloric acid, we added citric acid while stirring constantly. The complexation of magnetite cores with citrate molecules was accomplished by heating at 50 °C for 30 min. The particles were then magnetically separated and washed with distilled water to remove excess citric acid. For neutralization and particle stabilization, the pH value was increased stepwise while stirring up to 7.5 using 1 M potassium hydroxide. The particle dispersion was obtained at room-temperature using an Ultra Turrax (speed, 10 000 rpm; dispersion time, 2 min). Finally, the dispersion was filtered twice through glass fibers. A stable magnetic fluid of pH 7 was obtained (Figure 1a). The hydrodynamic diameter was 8.2 nm, and the width distribution was 8.6 nm as measured by dynamic light scattering (ZetaSizer 3000HS, Malvern Instruments Ltd, U.K.). This was also supported by transmission electron microscopy imaging (Figure 1b). The citrate coating leads to a negative surface charge of the SPIONs (zeta potential -50 mV, ZetaSizer 3000HS).

RBCs were collected from healthy volunteers and anticoagulated with ethylenediaminetetraacetate. Then the cells were washed three times with phosphate buffered saline (PBS, 300 mOsm, pH 8). For the loading procedure, 3 mL of packed RBCs and 4 mL magnetite nanoparticles were incubated under stirring in 100 mL hypoosmotic lysing buffer (Na_2HPO_4/NaH_2PO_4 , 20 mOsm, pH 8) at 4 °C for 1 h. To wash off the free hemoglobine and excess Fe_3O_4 nanopar-



Figure 2. Magnetite-loaded RBCs respond to an attached permanent magnet.

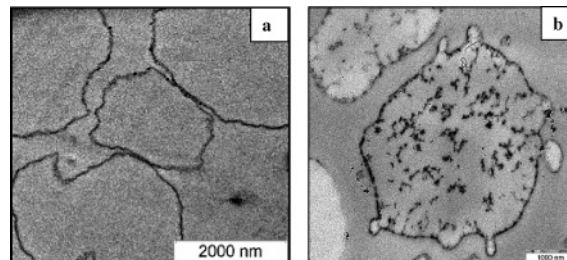


Figure 3. TEM pictures of (a) nonloaded control RBCs and (b) SPION-loaded RBCs. The control samples were stained with trypan blue before transferring them into ethanol in order to enhance the contrast.

ticles, we washed the RBCs with PBS using a stirred filtration cell (model 8200, 200 mL) with a MF membrane filter (3 μ m, Millipore GmbH, Schwalbach, Germany). The washed RBCs were resealed by incubation in 100 mL PBS at 37 °C for 1 h.

To prove the magnetic properties after loading, we placed the packed cells in a cuvette, attached a permanent magnet to the wall, and moved it upward slowly. As can be seen in Figure 2, the RBCs respond to the external magnetic field moving toward the attached magnet.

The magnetic response confirms interaction and attachment of SPIONs to the cells. However, it is important to know their distribution inside the cells and on their surface. For this purpose, we took TEM pictures of loaded and control RBCs. The control cells were treated in the same way as the loaded ones, incubating them in hypoosmotic buffer, but without SPIONs. The samples were cross-linked with 1% glutaraldehyde for 25 min, transferred into ethanol, embedded into methyl methacrylate containing 2,2'-azobis(2-methylpropionitrile) (AIBN), degassed, and polymerized at 60 °C overnight. Sections of 50–100 nm in thickness were prepared using an ultramicrotome (Leica ultracut UCT, Leica, Germany). The sections were then transferred onto a carbon film-coated copper grid and investigated by means of a transmission electron microscope (Zeiss EM 912 Omega) (Figure 3).

In the image of the control (Figure 3a), it can be seen that there are no particles inside the cells. The membrane is evenly stained because of the adsorption of the trypan blue dye. The loaded cells (Figure 3b) were not additionally stained, and the contrast on the image is caused only by the

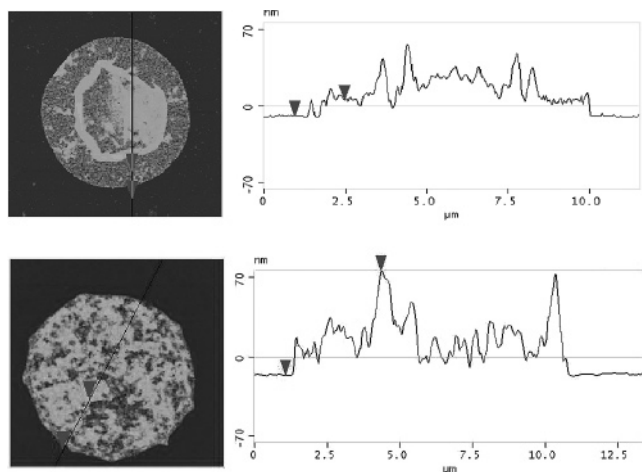


Figure 4. AFM images with height profiles of (a) control and (b) SPION-loaded cells.

SPIONs. The picture shows that they are located mostly inside the cells but also in the membrane. No SPIONs can be seen outside the cells, which means that they are stable entrapped in the inner volume of the cells despite the relatively aggressive sample preparation procedure for TEM imaging (see above). The sample preparation procedure could also be the reason for the agglomerates of particles seen inside the cells. However, they could also be formed earlier, during the encapsulation procedure caused by the interaction between the particles and the remaining hemoglobin.

The loading of the cells was also examined by atomic force microscopy (AFM). The samples have been prepared by applying a drop of the cell suspension onto a freshly cleaved mica substrate. After allowing the cells to sediment, the substrate was rinsed extensively in Millipore water and then dried under a gentle stream of nitrogen. The AFM images have been recorded at room temperature using a Nanoscope III Multimode AFM (Digital Instrument Inc., Santa Barbara, CA) in tapping mode. Microlithographed tips on silicon nitride (Si_3N_4) cantilevers with a force constant of 0.58 N/m (Digital Instrument Inc., Santa Barbara, CA) have been used. The images were processed by using the Nanoscope software. It can be seen that both control and loaded cells collapse because of the drying procedure but their appearance is completely different. Although the control cells are relatively

flat with some folds, the loaded cells show a grainy structure. The thickness of the dried cells was measured as the height difference between the support and the lowest point of a flat area of the cell profile. In the case of the control, the vertical distance of approximately 15 nm corresponds to the double membrane thickness of nonloaded cells (Figure 4a). In the case of magnetite-loaded cells (Figure 4b), the height difference between the support and the highest point representing the top of a SPION particle was measured. It can be seen that the presence of SPIONs in the loaded cell result in elevations of up to 94 nm.

The efficacy of loading was quantified measuring the SPION concentration of loaded cells by means of atomic absorption spectroscopy. Packed cells (500 μL) (SPION-loaded cells and hemolyzed cells without SPIONs) were boiled in 4500 μL of 37% HCl. After dissolution, the samples were diluted in aqua dest. and analyzed by an atomic absorption spectrometer (Perkin-Elmer 3100). The iron content of the nonloaded control cells was subtracted from the iron content of the loaded cells. The remaining iron content was the iron derived from the SPIONs. The SPION content inside the loaded cells was 0.01 wt %. This corresponds to an efficiency of approximately 5% for the hypoosmotic loading procedure described above.

Furthermore, we studied the magnetic properties of the loaded cells because they are crucial for applications in magnetic resonance imaging. A certain reduction of the relaxation times is needed to cause contrast enhancement in MRI. Therefore, we performed measurements by means of relaximetry. Native and SPION-loaded RBCs were diluted in PBS to a hematocrit (hct) of 25% and examined in a Bruker minispec Contrast Agent Analyzer (Bruker, Karlsruhe, Germany). The results are presented in Figure 5.

Both the longitudinal and the transverse relaxation times change dramatically. T1 decreases from 1750 ms for the native cells to 56 ms for the loaded ones and T2 from 210 ms to 12 ms, respectively. This corresponds to a reduction of 96.9% for T1 and 94.3% for T2, which is evidence of the fact that the SPION-loaded cells are suitable as MRI contrast agents.

Finally, the ability of loaded RBCs to enhance the contrast in MRI was tested in phantoms prepared as follows:

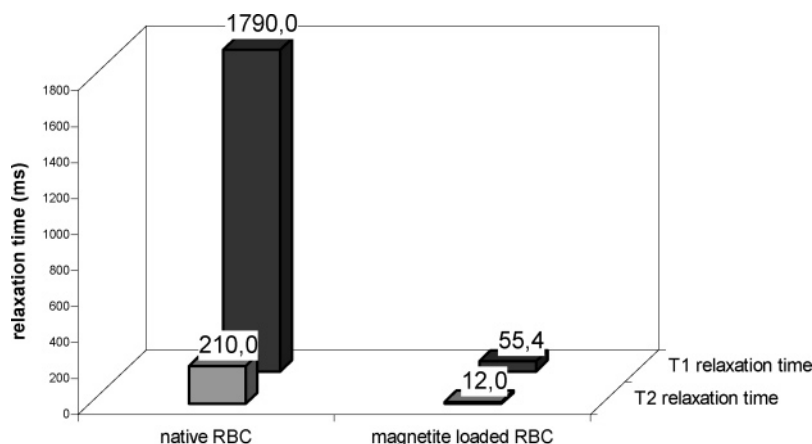


Figure 5. Relaxation times (T1 and T2) of native and SPION-loaded human RBCs.

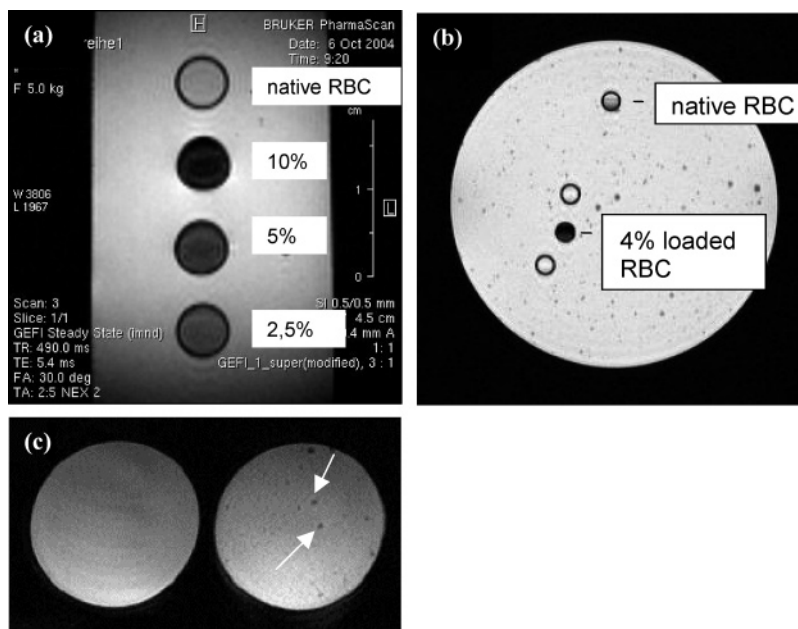


Figure 6. (a) MRI (Bruker Pharm Scan, Bruker, Karlsruhe, Germany) of the loaded RBCs. Top down: whole blood and loaded RBCs in whole blood, 10, 5, and 2.5%; (b) MRI (Bruker Pharm Scan, RARE sequence, Spin Echo, T2) of native and loaded RBCs (4%); (c) single-cell MRI at 3.0 T (Signa 3T94, GE Healthcare, Milwaukee, WI, method: 2D_GE_T2*_tra.) of native RBCs (left) and loaded RBCs (see arrow, right) (1000 cells/mL).

Magnetite-loaded RBCs were diluted to final concentrations of 10, 5, and 2.5% with whole blood. The samples were filled in 2 mL Eppendorf tubes and embedded in 20% gelatin. To simulate small blood vessels, we examined phantoms with a diameter of 1 mm. For this purpose, loaded RBCs were mixed to a final volume concentration of 4% with native RBCs. This is equivalent to a 10% content of loaded cells related to the total number of RBCs, which is the highest concentration of loaded RBCs that can be transfused in vivo. The RBC suspension was filled into clinitubes, and we embedded the tubes in 20% gelatin. In addition, we examined whether single loaded cells could be visualized by MRI. Loaded and native cells were embedded separately in eppendorf tubes filled with 20% gelatin at a concentration of 1000 cells/mL.

The obtained MR images are shown in Figure 6. It can be seen that even a 2.5% concentration of loaded cells in native cells shows a higher contrast than the native cells alone (Figure 6a). A concentration of 4% in a small-diameter phantom (1 mm) showed a clearly enhanced contrast (Figure 6b). This demonstrates that the loaded cells can be used for contrast enhancement in small blood vessels. Finally, it was possible to visualize individual loaded cells by means of a clinical 3T scanner (Figure 6c), whereas native cells could not be detected. The in vivo detection of single cells is a quality criterion for the loading procedure. This high in vitro resolution is very important because it indicates that a relatively small number of loaded cells will be sufficient to contrast specific sites of interest in vivo.

With this work, we demonstrate that citrate-coated SPIONs can be loaded into RBCs. The nanoparticles are distributed inside the cells, but they are also strongly attached to the membrane. The obtained amount of 0.01 wt % SPIONs

inside the cells is sufficient to obtain strong contrast enhancement even in small vessels. The method was reproducible in more than 10 separate preparations.

A modified cell surface due to attached SPIONs might be a restriction for the application of this loaded cells in vivo because it could activate elimination of the loaded cells by the immune system. Experiments are on the way to examine different coatings of SPIONs in order to reduce their binding to the outer membrane surface.

Acknowledgment. We thank Ms. Fabian, Institut für Chemie, HU Berlin, for the atomic absorption readings. We are grateful to Ms. Heilig and Ms. Pietschke, MPI of Colloids and Interfaces for AFM and TEM imaging. This work was financially supported by grant 2005-249 of the Charité-Universitätsmedizin Berlin.

References

- (1) Weinmann, H. J.; Laniado, M.; Mutzel, W. *Physiol. Chem. Phys. Med. NMR* **1984**, *16*, 167–72.
- (2) Wu, E. X.; Tang, H.; Jensen, J. H. *NMR Biomed.* **2004**, *17*, 478–83.
- (3) Wang, Y. X.; Hussain, S. M.; Krestin, G. P. *Eur. Radiol.* **2001**, *11*, 2319–31.
- (4) Taupitz, M.; Wagner, S.; Schnorr, J.; Kravec, I.; Pilgrimm, H.; Bergmann-Fritsch, H.; Hamm, B. *Invest. Radiol.* **2004**, *39*, 394–405.
- (5) Magin, R.L.; Bacic, G.; Niesman, M. R.; Alameda, J. C., Jr.; Wright, S. M.; Swartz, H. M. *Magn. Reson. Med.* **1991**, *20*, 1–16.
- (6) Saini, S.; Stark, D. D.; Hahn, P. F.; Wittenberg, J.; Brady, T. J.; Ferrucci, J. T., Jr. *Radiology* **1987**, *162*, 211–6.
- (7) Hemmingsson, A.; Carlsten, J.; Ericsson, A.; Klaveness, J.; Sperber, G. O.; Thuomas, K. A. *Acta Radiol.* **1987**, *28*, 703–5.
- (8) Schmidt, H. In *Klin. Kernspintomographie*; Lissner, S., Ed.; Enke: Stuttgart, 1987.
- (9) Abramjuk, C. *Magnetresonanztomographische und Histologische Untersuchungen zum Biologischen und Physikalischen Verhalten eines Monomer Stabilisierten Superparamagnetischen Kontrastmittels*

- für die Magnetresonanztomographie am Modell der Ratte*, in *Veterinärmedizin*; Freie Universität Berlin: Berlin, 2001; p 149.
- (10) Magnani, M.; Rossi, L.; Fraternale, A.; Bianchi, M.; Antonelli, A.; Crinelli, R.; Chiarantini, L. *Gene Ther.* **2002**, 9, 749–51.
- (11) Millan, C. G.; Marinero, M. L.; Castaneda, A. Z.; Lanao, J. M. *J. Controlled Release* **2004**, 95, 27–49.

- (12) Updike, S. J.; Wakamiya, R. T. *J. Lab. Clin. Med.* **1983**, 101, 679–91.
- (13) Kinoshita, K., Jr.; Tsong, T. Y. *Nature* **1978**, 272, 258–60.

NL0618501